A 14.6 billion degrees of freedom, 5 teraflops, 2.5 terabyte earthquake simulation on the Earth Simulator

[Extended Abstract]

Dimitri Komatitsch
Caltech
Pasadena, California, USA
komatits@gps.caltech.edu

Seiji Tsuboi*
IFREE, JAMSTEC
Yokohama, Japan
tsuboi@jamstec.go.jp

Chen Ji & Jeroen Tromp
Caltech
Pasadena, California, USA
jichen@gps.caltech.edu
jtromp@gps.caltech.edu

ABSTRACT

We use 1944 processors of the Earth Simulator to model seismic wave propagation resulting from large earthquakes. Simulations are conducted based upon the spectral-element method, a high-degree finite-element technique with an exactly diagonal mass matrix. We use a very large mesh with 5.5 billion grid points (14.6 billion degrees of freedom). We include the full complexity of the Earth, i.e., a three-dimensional wave-speed and density structure, a 3-D crustal model, ellipticity as well as topography and bathymetry. A total of 2.5 terabytes of memory is needed. Our implementation is purely based upon MPI, with loop vectorization on each processor. We obtain an excellent vectorization ratio of 99.3%, and we reach a performance of 5 teraflops (30% of the peak performance) on 38% of the machine. The very high resolution of the mesh allows us to perform fully three-dimensional calculations at seismic periods as low as 5 seconds.

1. INTRODUCTION

Modeling of the three-dimensional (3-D) seismic wave-speed structure of the Earth, the rupture process during a large earthquake, and propagation of resulting seismic waves is of considerable interest in seismology, because analyzing seismic wave propagation in the Earth is one of the few avenues of mapping the structure of the Earth's interior, based upon seismic tomography. Seismic waves resulting from earthquakes can be classified in two main categories: body waves, which propagate inside the medium and are of two types: compressional (pressure) waves, usually called P waves, and shear waves, usually called S waves; and surface waves, which travel along the surface of the medium and have an exponentially decreasing amplitude with depth. They are called Rayleigh or Love waves depending on their polarization relative to the direction of propagation. Seismic modeling has traditionally been performed using a combination of short-period body and long-period surface waves. Thus, the validation of 3-D Earth models and finite-source models requires the ability to calculate accurate theoretical seismograms (time series representing the three component of displacement at points located on the surface of the Earth), i.e., calculating broadband synthetic seismograms that contain both short-period body waves and long-period surface waves for a given 3-D Earth model.

The field of numerical modeling of seismic wave propagation in 3-D structures has significantly evolved in the last few years due to the introduction of the Spectral-Element Method (SEM), which is a high-degree version of the finite-element method that is very accurate for linear hyperbolic problems such as wave propagation, having very little intrinsic numerical dispersion. In addition, the mass matrix is exactly diagonal by construction, which makes it much easier to implement on parallel machines because no linear system needs to be inverted. The 3-D SEM was first used in seismology for local and regional simulations [8, 6, 17], and more recently adapted to wave propagation at the scale of the full Earth [2, 10, 11]. However, until recently, at the scale of the global Earth available computer resources intrinsically limited such large calculations. For instance, on a PC Beowulf Cluster with 150 processors, Komatitsch and Tromp [10] reached minimum seismic periods of 18 seconds (i.e. 1/18 Hz). Such periods are not short enough to capture important effects on wave propagation related to smaller-size 3-D heterogeneity in the Earth.

Here we implement the SEM on the Japanese Earth Simulator, the world's fastest supercomputer (see the Top500 list of supercomputers for details, `www.top500.org`), which opened in 2002 at the Japan Marine Science & Technology Center (JAMSTEC) in Yokohama, Japan. We show that on 38% of the machine we can simulate seismic waveforms accurately down to a minimum period of 5 seconds, i.e., almost a factor of 4 better than on our Beowulf cluster. (Note that one pays a factor of 16 in terms of numerical cost every time one wants to improve the resolution by a factor of 2, because the mesh needs to be doubled in the three directions of space, and in addition the time step needs to be divided by two in the fully-explicit conditionally-stable time integration scheme used in the SEM).

We include the full complexity of the 3-D Earth in our simulations, i.e., a three-dimensional (3-D) wave speed and density structure, a 3-D crustal model, ellipticity as well as topography and bathymetry [10, 11]. We also include the effect of the oceans on surface wave dispersion [11]. Synthetic waveforms at such high resolution (seismic periods of 5 seconds and above) allow us to perform direct comparisons of arrival times of various body wave

*To whom correspondence should be addressed

SC '03, November 15-21, 2003, Phoenix, Arizona, USA

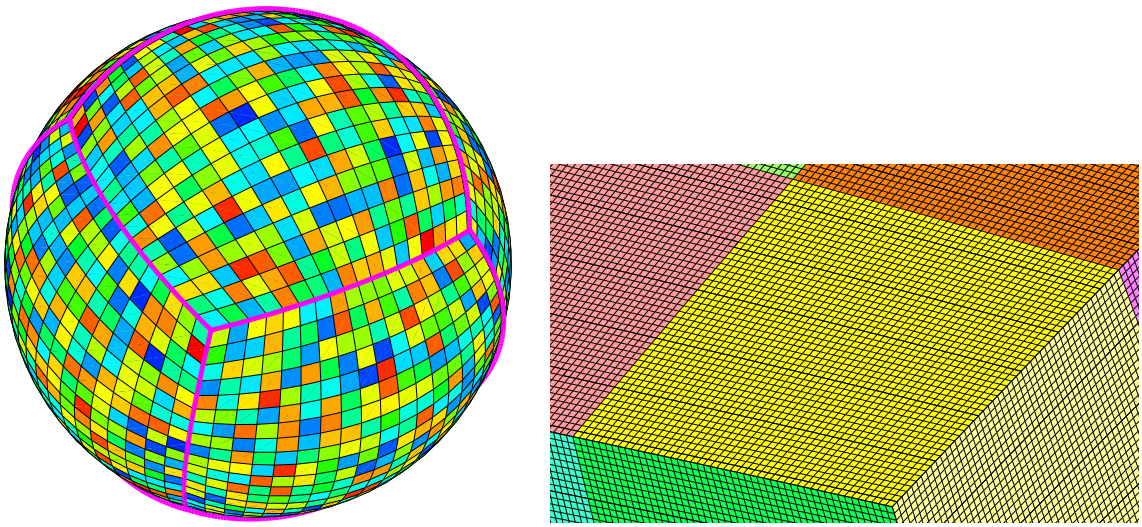

Figure 1: The SEM uses a mesh of hexahedral finite elements on which the wave field is interpolated by high-degree Lagrange polynomials on Gauss-Lobatto-Legendre (GLL) integration points. The left figure shows a global view of the mesh at the surface, illustrating that each of the six sides of the so-called 'cubed sphere' mesh is divided into 18 $\times$ 18 slices, shown here with different colors, for a total of 1944 slices (i.e., one slice per processor). The right figure shows a close-up of the mesh of 48 $\times$ 48 spectral-elements at the surface of each slice. Within each surface spectral element we use 5 $\times$ 5 = 25 GLL grid points, which translates into an average grid spacing of 2.9 km (i.e., 0.026°) on the entire Earth surface.

phases between observed and synthetic seismograms, which has never been accomplished before. Usual seismological algorithms, such as normal-mode summation packages that calculate quasi-analytical synthetic seismograms for one-dimensional (1-D) spherically symmetric Earth models [3], are typically accurate down to 8 seconds. In other words, the SEM on the Earth Simulator allows us to simulate global seismic wave propagation in fully 3-D Earth models at periods shorter than current seismological practice for simpler 1-D spherically symmetric models.

2. IMPLEMENTATION OF THE SPECTRAL-ELEMENT METHOD ON THE EARTH SIMULATOR

The SEM is based upon a weak formulation of the equations of motion, obtained after dotting the classical differential linear wave equation with a so-called test vector (in finite-element parlance) and integrating by parts over the volume of the model. The SEM leads to an exactly diagonal mass matrix, therefore no linear system needs to be inverted and the method lends itself well to calculations on large parallel machines with distributed memory, such as the Earth Simulator.

The SEM combines the flexibility of the finite-element method with the accuracy of the pseudospectral method. It uses a mesh of hexahedral finite elements on which the wave field is interpolated by high-degree Lagrange polynomials on Gauss-Lobatto-Legendre (GLL) integration points [12, 9, 10]. The mesh honors all first and second-order discontinuities in the reference Earth model [4]. In the mantle, crust and solid inner core of the Earth, we solve the anelastic seismic wave equation in terms of the displacement vector, whereas in the liquid outer core we solve the acoustic wave equation in terms of a fluid potential [10]. The SEM has been extensively benchmarked against semi-analytical reference solutions for 1-D reference Earth models in previous work [10, 11]. To represent the 3-D Earth, we use mantle model S20RTS [14], crustal model CRUST2.0 [1], and global topography and bathymetry model ETOPO5 (from the U.S. National Oceanic and Atmospheric Administration).

The Earth Simulator in Yokohama, Japan, has 640 8-processor compute nodes, for a total of 5120 processors. Each node has 16 gigabytes of shared memory, for a total of 10 terabytes of memory. Peak performance per node is approximately 64 gigaflops and total peak performance is approximately 40 teraflops. Because of the vector processor architecture, measured peak and sustained performance in the Top500 list of supercomputers (`www.top500.org`) are very close to theoretical performance, with measured $R_{\rm peak} = 41$ teraflops and $R_{\rm max}$ = 35.9 teraflops for the LINPACK benchmark. The reader can refer to [18] for more details about the hardware architecture of the Earth Simulator.

Figure 1 shows a global view of the spectral-element mesh at the surface of the Earth. The sphere is meshed using hexahedra only, based upon an analytical mapping from the six sides of a unit cube to a six-block decomposition of the surface of the sphere, which is called the 'cubed sphere' [16, 15, 2, 10]. The figure illustrates that each of the six sides of the 'cubed sphere' mesh is divided into 18 $\times$ 18 slices, shown with different colors, for a total of 1944 slices. We use 38 % of the machine (1944 processors, i.e., 243 nodes out of 640) and allocate one slice per processor. The figure also shows a close-up of the mesh of 48 $\times$ 48 spectral-elements at the surface of each slice. Within each surface element we use 5 $\times$ 5 = 25 GLL grid points, which translates into an average grid spacing of 2.9 km (i.e., 0.026°) at the surface. The total number of spectral elements in this mesh is 82 million, which corresponds to a total of 5.47 billion global grid points, since each spectral element contains $5 \times 5 \times 5 = 125$ grid points, but with points on its faces shared by neighboring elements. This in turn corresponds to 14.6 billion degrees of freedom (the total number of degrees of freedom is slightly less than 3 times the number of grid points because we solve for the three components of displacement everywhere in the mesh, except in the liquid outer core of the Earth where we solve for a scalar potential, as mentioned above).

Using this mesh, we can calculate synthetic seismograms that

are accurate down to seismic periods of 5 seconds. Such simulations use a total of approximately 2.5 terabytes of memory. As a comparison, we can simulate global wave propagation only down to seismic periods of 18 seconds on a three-year-old Caltech PC cluster computer with 150 processors (733 MHz Pentium-III) and 75 gigabytes of memory. The mesh files, created once and for all by our in-house parallel mesh generator, are stored on the Earth Simulator's large capacity tape system, to avoid having to recreate the mesh every time we start a new simulation (mesh creation and file saving takes of order 1 hour on 1944 processors, mainly because of the sorting routine required to create a global numbering from the local numbering of grid points in each elements, and to remove multiple entries in the list of common points between neighbors).

Our SEM solver is based upon a pure MPI implementation, combined with loop vectorization. We initially implemented a mixed MPI – OpenMP solution, using MPI between nodes (i.e., between blocks of 8 processors with shared memory), and using OpenMP inside each node. However, in practice, tests on a small number of processors gave a CPU time that was almost identical to a pure MPI run, and therefore we decided early on to permanently switch to an MPI implementation. We do not claim that this conclusion is general on the machine; it might well be specific to our SEM algorithm, in particular we did not try the mixed OpenMP – MPI solution on a large number of nodes. Other groups have successfully implemented algorithms based upon mixed OpenMP – MPI models on the Earth Simulator.

The SEM algorithm is not 'embarrassingly parallel', because of the need to assemble internal force contributions between neighboring slices, and because of the pattern of communications needed to assemble such slices on the edges and corners of the six blocks of the cubed-sphere mesh, as can be seen in Figure 1 (for instance the valence of most surface points is 4, but it is three at the corners of the six blocks). However, because the mass matrix is exactly diagonal, processors spend most of their time performing actual computations, and the amount of communications is comparatively small (but not negligible). Because of the regular mesh pattern in each of the six blocks of the cubed sphere, load balancing is very good by construction in our SEM algorithm.

Historically, our SEM code was initially developed in 1996 on a Thinking Machine CM-5, then ported to a Sun Enterprise using shared memory with compilation directives, and then to MPI on a Linux PC cluster. Therefore, it took no effort to parallelize the code on the Earth Simulator, because we already had a portable MPI implementation. The current package is written in Fortran95 + MPI, and contains approximately 40,000 lines of main source code. The original CM-5 code was written in Fortran77 with some Thinking Machine proprietary extensions similar to High-Performance Fortran (HPF). Therefore, the main effort in terms of maintaining the code occurred several years ago when we made the decision to permanently switch from HPF to MPI, first because we had to handle all the domain decomposition ourselves, and second because we had to parallelize the mesh generator in addition to the solver. For reasons related to performance, we use dynamic memory allocation in the mesh generator, but static allocation in the solver. Because all the arrays have a fixed size, the Fortran95 compiler can thus optimize the solver more aggressively. The only drawback is that we need to recompile the solver every time we change the size of the mesh.

Loop vectorization was more difficult issue to address. Performance critically depends on vectorization on the Earth Simulator. Unfortunately, our existing Fortran95 MPI source code could not be fully vectorized automatically by the compiler because of the fact that the main routines consist of matrix-vector products in each spectral element, but these elements, and therefore the related matrices and vectors, are very small ($5 \times 5 \times 5$ grid points as mentioned above). Therefore, these matrix operations are too small to be efficiently replaced by calls to a standard optimized library, such as BLAS, because the overhead is large. We therefore manually restructured and inlined most of these loops (in particular critical inner loops). The key issue was to reorder loop index variables to make sure that vector register access became continuous. Fortunately, only two small routines had to be rewritten (the code spends 80 to 90 percent of the CPU time in these critical routines, which are small in terms of source code size). After manual loop restructuring, all critical loops in the SEM code were fully vectorized, and we reached an excellent vectorization ratio of 99.3 %, measured using the "MPI Program Runtime Performance Information" system tool developed by NEC Corporation, and available on the Earth Simulator. The reader can refer to [18] for more details about how performance analysis is performed on the Earth Simulator.

I/O was not an issue in the context of our wave propagation simulation project, because we only output a small number of time series to record seismic motion (the three components of the displacement vector) at a small number of points at the surface of the mesh (the existing seismic recording stations). These time series (called 'seismograms') are then compared to recorded data from real earthquakes, as will be illustrated in the next section. This means that the amount of data saved by our SEM is negligible.

Using 1944 processors, a simulation of 60 minutes of actual seismic wave propagation accurate down to a period of 5 seconds requires about 15 hours of wall-clock time (using 50000 time steps of 72 ms each for the explicit time integration scheme of the SEM algorithm). Total performance of the code (again measured using the "MPI Program Runtime Performance Information" system tool developed by NEC Corporation and available on the Earth Simulator) was 5 teraflops, which is about one third of expected peak performance for this number of nodes (243 nodes $\times$ 64 gigaflops = 15 teraflops). This performance level is not as high as that reached by other applications on the Earth Simulator, mostly because of the short vector lengths involved in the matrix-vector products in the SEM algorithm. As mentioned above, each spectral-element contains $5 \times 5 \times 5 = 125$ points, which is about half the size of the vector registers on the Earth Simulator (256). As a result, loop operations performed at the level of the elements do not fully take advantage of the vector pipes.

Because the batch management system limits wall-clock time to 6 hours when using more than 1/3rd of the machine, we ran the total simulation in three sequential steps of 5 wall-clock hours each, based upon restart files saved to the large-capacity tape system.

3. SEISMIC WAVE PROPAGATION RESULTING FROM LARGE EARTHQUAKES IN THE FULL 3-D EARTH

We first simulate a deep magnitude 6.7 earthquake that occurred in Colombia on September 2, 1997, at a depth of 213 km. Because there are more than 120 seismic recording stations ('seismometers') now permanently installed worldwide, which gives us access to broadband records of the three components of displacement, we can perform a direct comparison between our synthetic seismograms and real data from recorded earthquakes. Such records are composed of compressional, shear and surface waves and their multiples reflected and converted in the layers of the Earth model, as mentioned previously.

3-D seismic models of the wave-speed structure of the Earth are traditionally built based upon a combination of travel-time anoma-

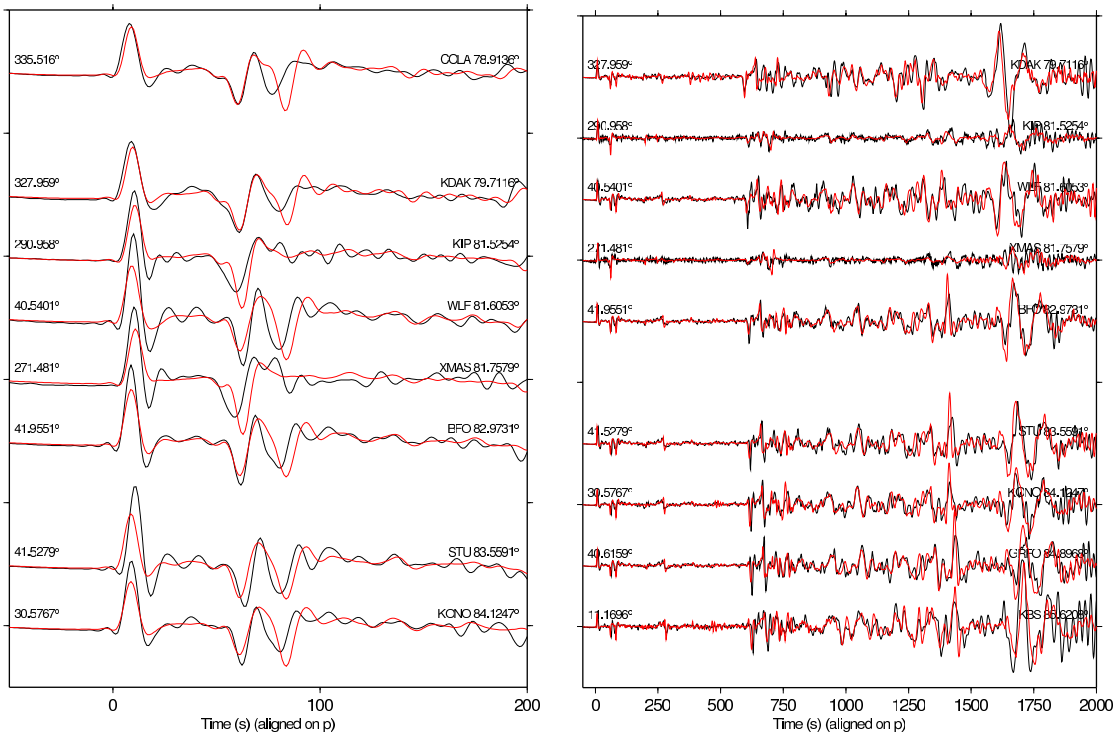

Figure 2: (Left) Broadband data and synthetic displacement seismograms for the 1997 Colombia earthquake bandpass-filtered with a two-pass four-pole Butterworth filter between periods of 5 and 150 seconds. Vertical component data (black) and synthetic (red) displacement seismograms aligned on the arrival time of the P wave are shown. For each set of seismograms the azimuth is printed above the records to the left, and the station name and epicentral distance are printed to the right. (Right) Similar seismograms at other seismic stations for a total duration of 2000 seconds instead of 200 seconds.

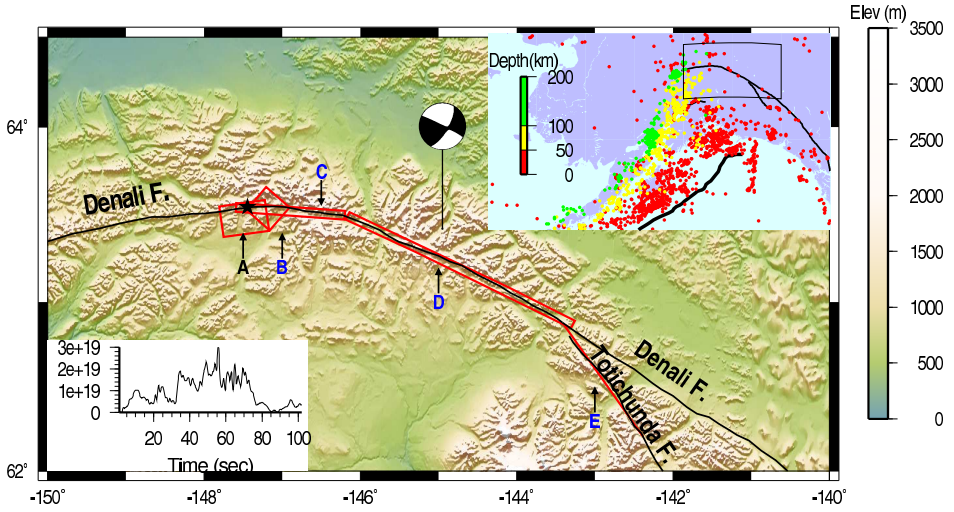

Figure 3: Fault geometry of the November 3, 2002, Denali, Alaska, earthquake. The top-right inset shows a map on which epicenters of past earthquakes determined by the International Seismological Center are color-coded according to hypocentral depth, and clearly show the Aleutian slab (subducting plate). The thick black line off the coast denotes the location of the Aleutian trench. The black box denotes the area of detail shown in the larger map, on which the Denali and Totichunda faults are labeled. The Harvard Centroid-Moment Tensor solution (from the standard Harvard earthquake catalog, `www.seismology.harvard.edu`), which describes the source of the earthquake as an equivalent moment tensor, is shown by the black-and-white beach ball. The five red boxes labeled A–E denote the surface projections of the five fault segments that were involved in the rupture. The earthquake started at the black star with a thrust event represented by fault planes A and B, which both have a 32-degree dip to the North, and Northwest, respectively. The rupture then proceeded eastward as strike-slip motion along the nearly vertical fault planes C, D and E, which is the main reason why large directivity effects are observed in North America, as illustrated in Figure 4. Segments C and D represent the main rupture along the Denali fault, whereas segment E represents the rupture along the Totichunda fault. The average moment-rate function is plotted as a function of time in the bottom left corner of the map.

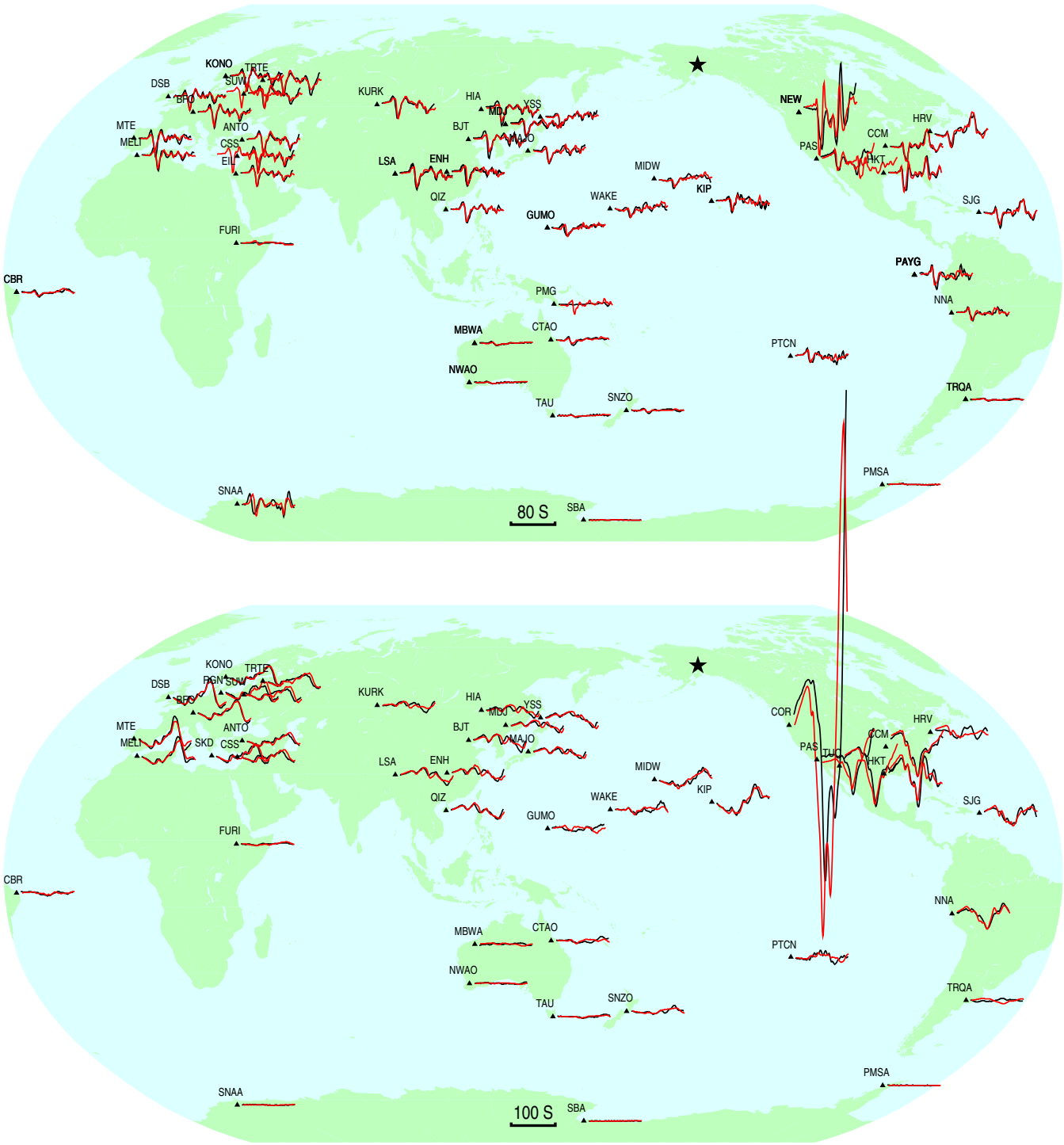

Figure 4: Maps on which stations in the Global Seismographic Network, which recorded displacement seismograms for the 2002 Alaska earthquake, are labeled and denoted by black triangles. To the right of each station the data are shown in black and the 3-D SEM synthetic seismograms in red. Both data and synthetic seismograms are bandpass-filtered with a two-pass six-pole Butterworth filter between periods of 5 and 150 seconds. The black star denotes the epicenter, and the black bar at the bottom denotes the time scale. Both data and synthetic seismograms are multiplied by the inverse of the body-wave geometrical spreading factor in an attempt to remove effects associated with epicentral distance. Top: P wave displacement on the vertical component. Bottom: S wave displacement on the transverse component. To compare the P- and S-wave amplitudes in the two figures the S waves need to be multiplied by a factor of four.

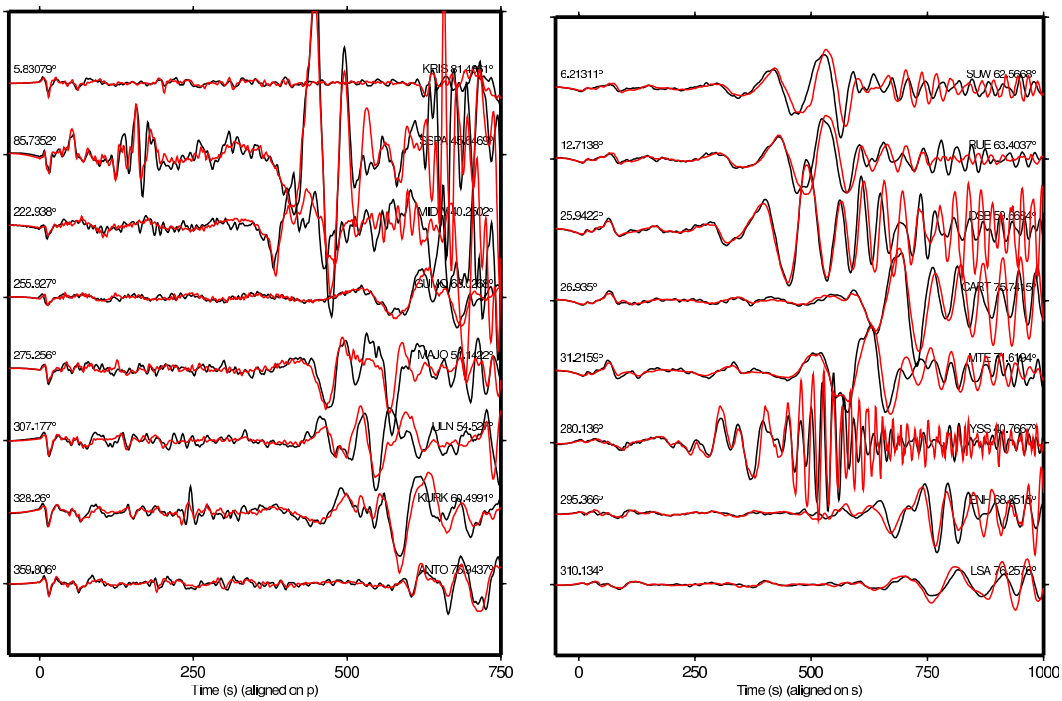

Figure 5: Broadband data and synthetic displacement seismograms for the 2002 Alaska earthquake, bandpass-filtered with a two-pass four-pole Butterworth filter between periods of 5 and 150 seconds. Left: vertical component data (black) and synthetic (red) displacement seismograms aligned on the arrival time of the P wave. Right: transverse component data (black) and synthetic (red) displacement seismograms aligned on the arrival time of the S wave. For each set of seismograms the azimuth is plotted above the records to the left, and the station name and epicentral distance are plotted to the right. The transverse component seismograms need to be multiplied by a factor of ten to compare them with the vertical component seismograms in terms of amplitude.

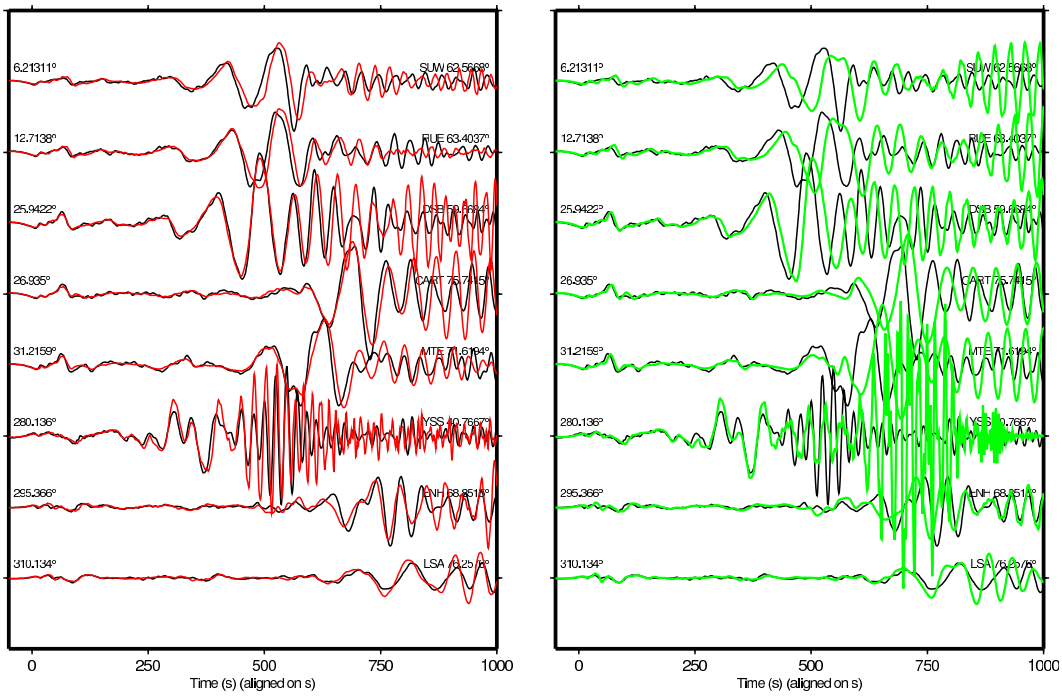

Figure 6: Broadband data and synthetic seismograms bandpass-filtered with a two-pass four-pole Butterworth filter between periods of 5 and 150 seconds. The transverse component of displacement is displayed. Left: data (black) and 3-D SEM synthetic seismograms (red) aligned on the arrival time of the S wave. Right: data (black) and 1-D synthetic seismograms for the spherically-symmetric reference Earth model PREM (green). The fit is significantly improved by the 3-D model. For each set of seismograms the azimuth is plotted above the records to the left, and the station name and epicentral distance are plotted to the right.

lies of short-period body waves and long-period surface waves. However, independent validation of such existing 3-D Earth models has never been attempted before, by lack of an independent numerical way of computing the seismic response in such models. Figure 2 shows the first attempt to verify such agreement; we compare the vertical component of displacement from synthetic seismograms and observed records for several seismic recording stations with an epicentral distance of about 75 to 85 degrees. The first peaks in these traces are the direct P waves. Because the Colombia earthquake was a deep event (located at a depth of 213 km), two so-called 'depth phases' are present in the records after the P arrivals. The first one is called the pP phase, which means that the P wave from the hypocenter first travels upward and then reflects off the surface of the Earth as a compressional wave. The second phase is called sP, which means that the S wave from the hypocenter first travels upward and reflects at the surface of the Earth and then propagates to the seismic station as a converted P wave.

The agreement between the synthetic seismograms and observed records for the P and pP phases in terms of arrival time is excellent for these stations, which means that the 3-D seismic P-wave speed model used in this simulation [14] is accurate. Therefore, our simulation demonstrates that this 3-D model represents the general picture of the Earth's interior fairly well. However, the arrival time for the sP phase is not as good for these stations, which in turn shows that the S-wave speed structure of this model is not as accurate around the earthquake epicenter region. This information could be directly used to further improve the current 3-D seismic wave speed model. Figure 2 also compares longer records of about 30 minutes of vertical component synthetic and observed seismograms. These records show that for most stations within this epicentral distance range both arrival times and amplitudes of body and surface waves are generally well reproduced by our current 3-D seismic wave speed model.

Next, we wish to model effects caused by the rupture propagating along a finite-size fault on the amplitudes of seismic waves for large earthquakes. We therefore simulate a very large recent earthquake that occurred in Alaska on November 3, 2002 (magnitude 7.9, at a depth of 15 km). This event is the largest strike-slip earthquake in North America since the very destructive April 18, 1906, San Francisco earthquake. (A strike-slip earthquake is an earthquake in which the two edges of the fault move in opposite directions in a horizontal fashion). It ruptured 220 km of the Denali fault in Central Alaska [5], in five distinct fault segments (Figure 3). As a comparison, the 1906 San Francisco earthquake also had a magnitude of approximately 7.9, and ruptured 430 km of the San Andreas fault from northwest of San Juan Bautista to Cape Mendocino.

Results of our simulations are shown in Figures 4 and 5. Because of the fact that the main rupture occurred in a southeasterly direction along large finite-size fault segments [13, 7], recorded seismograms show significantly enhanced ground motions toward the conterminous United States for both body (i.e., compressional and shear) and surface waves. Such an effect is called 'seismic directivity'. To define the finite-size fault model in our numerical simulations and model this strong directivity effect, we approximate it by a set of 475 sub-events of size 4 km $\times$ 5 km. In Figure 4 we show the results of the simulation for P and S waves filtered at periods between 5 and 150 seconds. The largest P and S wave arrivals are observed in North America because of the directivity. Figure 5 shows 12 minutes of vertical component displacement seismograms aligned on the arrival time of the P wave, and 17 minutes of transverse component displacement seismograms aligned on the arrival time of the S wave. The transverse component of displacement has an amplitude that is typically ten times larger than the vertical component. This reflects the predominantly strike-slip nature of the event. For reference, the same transverse component data are compared to SEM synthetic seismograms for the spherically-symmetric Earth model PREM [4] in Figure 6. The fit is significantly improved by the 3-D model.

4. CONCLUSIONS AND PERSPECTIVES

The Earth Simulator has allowed us to reach unprecedented resolution for the simulation of seismic wave propagation resulting from large earthquakes in the 3-D Earth. The results show that given a detailed earthquake source model, precise models of the Earth's mantle and crust, a precise numerical technique, such as the SEM, and a large computer, seismic waveforms generated by large earthquakes propagating through heterogeneous Earth models, which span an amplitude range that covers several orders of magnitude and a few decades in frequency, can be accurately modeled. In particular, we have successfully attempted for the first time an independent validation of an existing 3-D Earth model. Such 3-D calculations on the Earth Simulator reach shorter periods than quasi-analytical 1-D spherically-symmetric solutions that are current practice in seismology.

In the near future, the synthetic seismic waveform-modeling tool presented in this work will allow us to further investigate and improve existing Earth models. Because large earthquakes generally occur in subduction zones, where seismic wave-speed structure is more complex and intrinsically 3-D because of the subducting oceanic plate, this tool should also be effective for modeling the source rupture process of large earthquakes.

5. ACKNOWLEDGMENTS

All the simulations were performed at the Earth Simulator Center of JAMSTEC by S. T. Broadband seismogram data used in this study were obtained from the IRIS Data Management Center (`www.iris.washington.edu`). Three of the authors (D. K., C. J. and J. T.) were funded in part by the U.S. National Science Foundation. S. T. was funded by a Grant-in-Aid for Scientific Research (KAKENHI 13640426) from the Japan Society for the Promotion of Science. We thank four anonymous reviewers for comments that improved the manuscript. We also thank Brian Savage from Caltech for providing software that plots seismograms on maps.

6. REFERENCES

[1] C. Bassin, G. Laske, and G. Masters. The current limits of resolution for surface wave tomography in North America. *EOS*, 81:F897, 2000.

[2] E. Chaljub. *Modélisation numérique de la propagation d'ondes sismiques en géométrie sphérique: application à la sismologie globale (Numerical modeling of the propagation of seismic waves in spherical geometry: applications to global seismology)*. PhD thesis, Université Paris VII Denis Diderot, Paris, France, 2000.

[3] F. A. Dahlen and J. Tromp. *Theoretical Global Seismology*. Princeton University Press, Princeton, 1998.

[4] A. M. Dziewonski and D. L. Anderson. Preliminary reference Earth model. *Phys. Earth Planet. Inter.*, 25:297–356, 1981.

[5] D. Eberhart-Phillips, P. J. Haeussler, J. T. Freymueller, A. D. Frankel, C. M. Rubin, P. Craw, N. A. Ratchkovski, G. Anderson, G. A. Carver, A. J. Crone, T. E. Dawson, H. Fletcher, R. Hansen, E. L. Harp, R. A. Harris, D. P. Hill,

S. Hreinsdottir, R. W. Jibson, L. M. Jones, R. Kayen, D. K. Keefer, C. F. Larsen, S. C. Moran, S. F. Personius, G. Plafker, B. Sherrod, K. Sieh, N. Sitar, and W. K. Wallace. The 2002 Denali fault earthquake, Alaska: a large magnitude, slip-partitioned event. *Science*, 300:1113–1118, 2003.

[6] E. Faccioli, F. Maggio, R. Paolucci, and A. Quarteroni. 2D and 3D elastic wave propagation by a pseudo-spectral domain decomposition method. *J. Seismol.*, 1:237–251, 1997.

[7] C. Ji, D. V. Helmberger, and D. J. Wald. Preliminary slip history of the 2002 Denali earthquake. *EOS Trans. AGU.*, 83, 2002.

[8] D. Komatitsch. *Méthodes spectrales et éléments spectraux pour l'équation de l'élastodynamique 2D et 3D en milieu hétérogène (Spectral and spectral-element methods for the 2D and 3D elastodynamics equations in heterogeneous media)*. PhD thesis, Institut de Physique du Globe, Paris, France, 1997.

[9] D. Komatitsch and J. Tromp. Introduction to the spectral-element method for 3-D seismic wave propagation. *Geophys. J. Int.*, 139:806–822, 1999.

[10] D. Komatitsch and J. Tromp. Spectral-element simulations of global seismic wave propagation-I. Validation. *Geophys. J. Int.*, 149:390–412, 2002.

[11] D. Komatitsch and J. Tromp. Spectral-element simulations of global seismic wave propagation-II. 3-D models, oceans, rotation, and self-gravitation. *Geophys. J. Int.*, 150:303–318, 2002.

[12] D. Komatitsch and J. P. Vilotte. The spectral-element method: an efficient tool to simulate the seismic response of 2D and 3D geological structures. *Bull. Seismol. Soc. Am.*, 88(2):368–392, 1998.

[13] R. A. Page, G. Plafker, and H. Pulpan. Block rotation in east-central Alaska: a framework for evaluating earthquake potential? *Geology*, 23:629–632, 1995.

[14] J. Ritsema, H. J. Van Heijst, and J. H. Woodhouse. Complex shear velocity structure imaged beneath Africa and Iceland. *Science*, 286:1925–1928, 1999.

[15] C. Ronchi, R. Ianoco, and P. S. Paolucci. The "Cubed Sphere": a new method for the solution of partial differential equations in spherical geometry. *J. Comput. Phys.*, 124:93–114, 1996.

[16] R. Sadourny. Conservative finite-difference approximations of the primitive equations on quasi-uniform spherical grids. *Monthly Weather Review*, 100:136–144, 1972.

[17] G. Seriani. 3-D large-scale wave propagation modeling by a spectral element method on a Cray T3E multiprocessor. *Comput. Methods Appl. Mech. Engrg.*, 164:235–247, 1998.

[18] S. Shingu, H. Takahara, H. Fuchigami, M. Yamada, Y. Tsuda, W. Ohfuchi, Y. Sasaki, K. Kobayashi, T. Hagiwara, S.-I. Habata, M. Yokokawa, H. Itoh, and K. Otsuka. A 26.58 teraflops global atmospheric simulation with the spectral transform method on the Earth Simulator. *Proceedings of the ACM/IEEE Supercomputing SC'2002 conference*, 2002. Published on CD-ROM and at www.sc-conference.org/sc2002.